JGR Atmospheres

RESEARCH ARTICLE
10.1029/2020JD034364

The Limpopo Low-Level Jet: Mean Climatology and Role in Water Vapor Transport

Zachary D. Spavins-Hicks[1], **Richard Washington**[1], **and Callum Munday**[1]

[1]Climate Research Lab, School of Geography and the Environment, University of Oxford, Oxford, UK

Key Points:

- A nocturnal low-level jet forms on 80.9% of days in the Limpopo Basin
- The annual cycle of jet strength is unimodal, peaking in October with average maximum windspeeds of 15.8 $m.s^{-1}$
- Water vapor advected through the Limpopo Channel increases by 1.04×10^{12} kg each night during the strongest jet events in early summer

Supporting Information:

Supporting Information may be found in the online version of this article.

Correspondence to:

Z. D. Spavins-Hicks,
zachary.spavins-hicks@ouce.ox.ac.uk

Citation:

Spavins-Hicks, Z. D., Washington, R., & Munday, C. (2021). The Limpopo low-level jet: Mean climatology and role in water vapor transport. *Journal of Geophysical Research: Atmospheres*, *126*, e2020JD034364. https://doi.org/10.1029/2020JD034364

Received 7 DEC 2020
Accepted 4 AUG 2021

Abstract Low-level jets (LLJs) are well established as critical features of regional climates globally. However, across sub-Saharan Africa, LLJs have received relatively little attention, in part due to a lack of data. Utilizing high-resolution reanalysis data, this paper develops the first climatology of a neglected feature of the southern African circulation – the Limpopo LLJ – and investigates its role in delivering water vapor to the continental interior. We demonstrate that the LLJ has a clear diurnal cycle and is a regular feature of the circulation throughout the year, forming on 80.9% of days. The pressure gradient between southern Mozambique and the continental interior acts as a first-order control on the annual cycle of jet strength, which peaks in October, achieving average maximum windspeeds of 15.8 $m.s^{-1}$ at the core. Water vapor transport follows the same clear diurnal cycle, with at least 72% occurring over 18:00–08:00, and is closely related to jet strength: On average the strongest jet events advect 1.04×10^{12} kg (1.02×10^{12} kg) more moisture each night than the weakest in October-December (January-March). Strong jet events are typically linked to ridging anticyclones along the east coast of South Africa and are associated with increased rainfall in central and southern Botswana and northern South Africa the following day.

1. Introduction

Low-level jets (LLJs) are capable of transporting vast amounts of moisture between tropical and subtropical regions (e.g., Algarra et al., 2019; Gimeno et al., 2016; Ramos et al., 2019; Rife et al., 2010) and hence play a key role in configuring both the extremes and mean states of regional climates across the world. While the diurnal cycle of wind in Africa has attracted interest for nearly a century (e.g., Farquharson, 1939), LLJs across the continent have received notably less attention than elsewhere. Saharan LLJs have been the subject of targeted field campaigns due to their prominence as dust entrainment mechanisms (e.g., Allen & Washington, 2014; Washington et al., 2006), whereas comparatively little is known about LLJs in sub-Saharan Africa largely due to a lack of data. The advent of high-resolution reanalysis products in recent years offers an unrivalled amount of data with which these features can be investigated and has allowed significant progress to be made particularly in understandings of the Turkana Jet (Nicholson, 2016) and Benguela Coast LLJ (Nicholson, 2010; Patricola & Chang, 2017). In this study, we provide a first climatology for the LLJ forming across the Limpopo River Basin and eastern Botswana and investigate its relationship with regional climate.

The importance of African LLJs for moisture transport and the distribution of rainfall across the continent is emerging. In East Africa, Nicholson (2016) and Vizy and Cook (2019) link the Turkana LLJ to local aridity: the jet enhances divergence, suppressing rainfall in the channel while transporting moisture downstream, fueling rainfall over eastern South Sudan. Munday et al. (2021) demonstrate that the transport of Indian Ocean water vapor to the continental interior occurs mainly by a series of LLJs that form in valleys in the East African Rift System. The relationship between low-level divergence, moisture export and suppression of local rainfall observed in the Turkana Channel is also seen at interannual timescales in the case of the Zambezi and Malawi jets (Munday et al., 2021). The southernmost LLJ across the Rift System is found in the Limpopo Basin.

The Limpopo Basin stands out as a drought corridor (Thoithi et al., 2021) and has long been considered "the most conspicuous climatic peculiarity in southern Africa" (Trewartha, 1981:165, Figure 1c). Despite close proximity to the Agulhas Current and moisture reaching the basin from the South Atlantic, southwest, subtropical and tropical Indian Ocean basins (Rapolaki et al., 2020), the dry, subhumid conditions of the

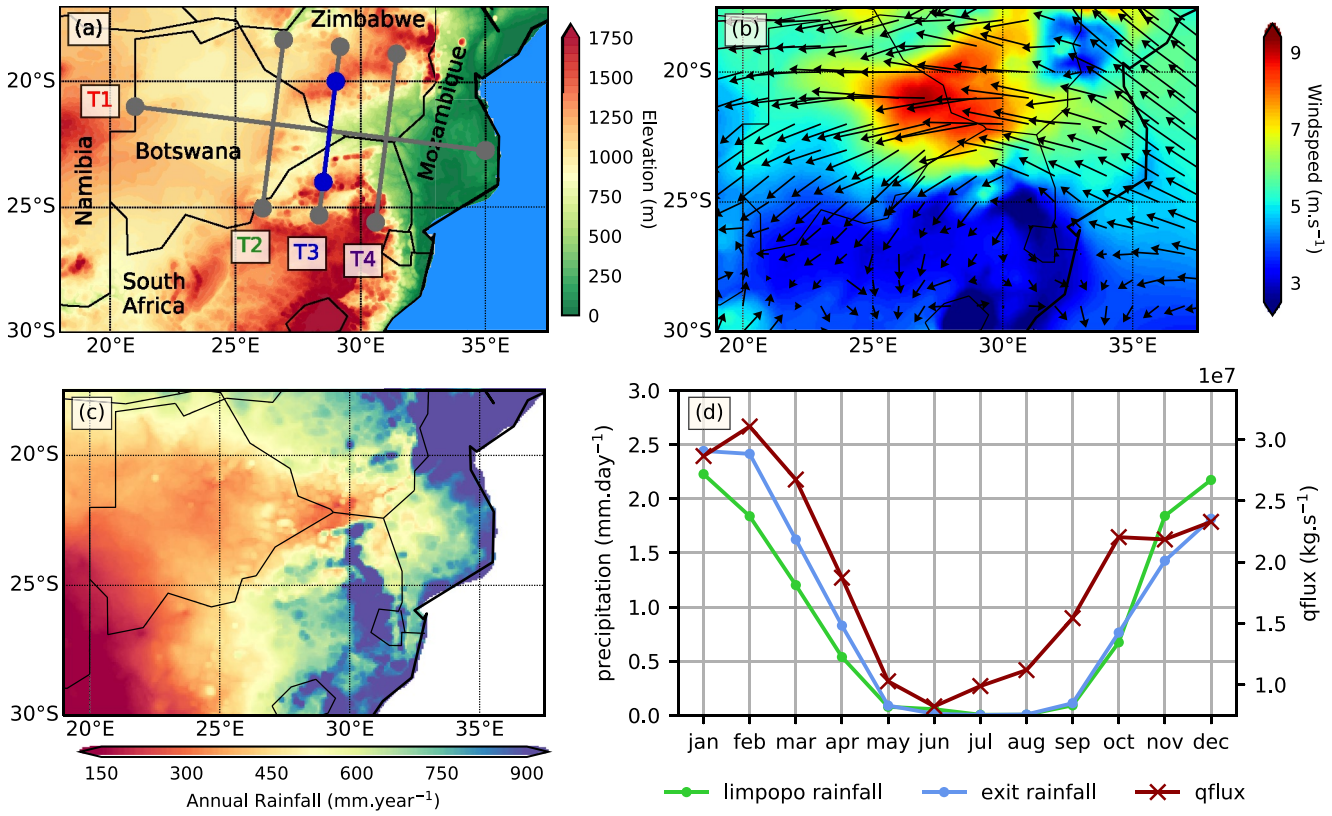

Figure 1. (a) The Limpopo River Basin topography (USGS–GTOPO30) in m showing the jet axis (T1) and perpendicular transects T2: interior, T3: head of Limpopo Valley and T4: Valley entrance. The blue section of T3 is used to calculate jet-related moisture transport. (b) Maximum annual mean windspeed (m.s^{-1}) over 1000-825 hPa at local midnight. (c) Average annual rainfall (mm.yr^{-1}). (d) Annual cycle of rainfall for the Limpopo Valley (green) and jet exit region (blue) in mm. day^{-1}, and annual cycle of moisture transport across the indicated portion of T3 (red; kg.s^{-1}).

continental interior extend almost to the east coast (Figure 1c). Nevertheless, warm sea surface temperatures (SSTs) nearby ensure that the atmosphere over eastern regions is conducive to the development of potentially severe convective environments throughout the summer (Blamey et al., 2017), so a substantial proportion of summer rainfall in this otherwise arid area occurs during intense spells–leaving the basin prone to both severe drought and floods. Mesoscale-convective complexes (MCCs) account for 8%–16% of summer rainfall (Blamey & Reason, 2013; Rapolaki et al., 2019), tropical-temperate troughs (TTTs) for 30%–50% (Hart et al., 2013; Rapolaki et al., 2019) and Indian Ocean cyclones can create extreme flooding events if they reach land (Reason, 2017).

While southern Africa has been identified as a potential region of frequent jet activity (Stensrud, 1996) and it has been speculated that jets are important for supplying moisture to the continental interior (Blamey & Reason, 2009, 2012; Cook et al., 2004), the structure of the Limpopo Jet is yet to be examined in detail. Global analyses (Algarra et al., 2019; Rife et al., 2010) have consolidated isolated observational records (as summarized by Zunckel et al., 1996), confirming the existence of a nocturnal LLJ across the Limpopo region. These studies generally label it the Botswana Jet; while jet activity extends into eastern Botswana, we opt for the Limpopo LLJ, consistent with Munday et al. (2021), due to its clear connection to the basin's topography. Tropical easterlies accelerate over the low-lying floodplains of Mozambique, strengthening as they pass through the steep-sided Limpopo Valley (i.e., the Bernoulli Effect) – as evident in the annual mean wind field at local midnight (Figure 1b).

The annual cycle of water vapor transport through the valley peaks in February (Munday et al., 2021) – closely resembling the annual cycle of rainfall (Figure 1d). Moisture supplied by a strong low-level easterly flow has been linked to heavy rainfall events in the region (Cook et al., 2004; Singleton &

Table 1
Characteristics of the Limpopo LLJ as Presented by Rife et al. (2010) and Algarra et al. (2019)

	Study	
Characteristic	Rife et al. (2010)	Algarra et al. (2019)
Dataset	NCAR MM5	ERA-Interim
Location of core	(32.8°E, 23.6°S)	(18°E, 26°S)
Windspeed at core	11.3 $m.s^{-1}$	9.0 $m.s^{-1}$
Jet onset time	17:00 LST	00:00 LST
Cessation time	01:00 LST	05:00 LST

Reason, 2006). Studies suggest that the jet may indeed be important for rainfall over the interior, linking it to the deliverance of South West Indian Ocean (SWIO) moisture toward the South Africa-Namibia-Botswana border intersection with an additional branch extending toward the Congo Basin (Algarra et al., 2019), as well as suggesting a relationship between jet strength and drought (Gimeno et al., 2016) and extreme nocturnal rainfall (Monaghan et al., 2010). However, neither the annual cycle nor the diurnal variability of the jet have been considered in detail, and the jet-related moisture transport has not been quantified. There is also considerable discrepancy in core location, windspeed and diurnal cycle emerging from key global studies considering the jet (Table 1). Thus, questions remain over its climatology and variability, in addition to its potential link to the basin's "problem climate" (Trewartha, 1981).

Before exploring the role the LLJ plays in regional climate it is important to establish the jet's climatology and variability. Therefore, this study addresses three main questions:

1. How does the vertical profile of windspeed vary throughout the day across the Limpopo Basin?
2. How does the LLJ vary at annual and intraseasonal timescales and what drives this variability?
3. What role does the LLJ play in moisture transport and how does this relate to regional precipitation?

The remainder of this paper is structured as follows. Section 2 outlines the data sources and approaches used. The analysis begins by examining the diurnal cycle of windspeed and its vertical structure throughout the year (Section 3). Section 4 investigates variability of the jet at intraseasonal timescales by imposing a series of criteria to categorize jet strength. Section 5 then uses this framework to explore the jet's role in moisture transport during austral summer. We conclude in Section 6.

2. Data and Methods

We use the latest ECMWF reanalysis dataset–ERA5 – for all atmospheric data across the period 1979–2018 (Hersbach et al., 2018a, 2018b). With grid spacings of 0.25 ° × 0.25 °, the mesoscale drivers responsible for the jet are more likely to be adequately captured than in coarser products, while the availability of hourly data permits a complete investigation of the diurnal cycle. All times presented are local (UTC+2). To estimate rainfall, we use the daily high-resolution Climate Hazards Group InfraRed Precipitation with Station data (CHIRPS) product (Funk et al., 2015) over 1981–2018.

As the time of maximum windspeed varies across the basin, sampling jet strength at a fixed time stands to induce biases to jet extent and core location. Thus, we take the maximum windspeed over 18:00–08:00 recorded across 925–800 hPa to represent daily jet strength. This calculation is performed for every grid cell. To determine monthly locations of the jet core, we select the maximal value of the monthly mean over (25°E, 20°S)–(34°E, 24°S).

We calculate water vapor transport associated with the Limpopo Jet in Section 5 following the approach used by Munday et al. (2021) – summing the scalar of moisture flux from the surface to 800 hPa normal to the indicated portion of transect T3 (Figure 1a) as follows:

$$Q = -\sin\theta \int_{P_S}^{800} qu\frac{dP}{g} + \cos\theta \int_{P_S}^{800} qv\frac{dP}{g}$$

where $\theta = \arctan\left(\frac{ly}{lx}\right)$, ly and lx are the latitude and longitude segments of transect T3, q is specific humidity, u and v are the zonal and meridional components of wind respectively, P is pressure, P_S is surface pressure and g is Earth's gravitational acceleration. Q is then interpolated to transect T3 and grid cells summed to give the total qflux. Units are $kg.s^{-1}$.

3. Climatology of the Limpopo LLJ

This section builds a climatology of the Limpopo Jet throughout the year by considering the vertical structure and diurnal cycle of windspeed across the Limpopo Basin.

3.1. Characteristics of Low-Level Circulation Over the Limpopo Basin

Throughout the year, average nocturnal maximum windspeeds >10m.s^{-1} are recorded in the Limpopo Valley over 925-800 hPa. From September-April, the low-level circulation over southern Mozambique comprises easterlies, which gain a greater meridional component as summer progresses and the Mozambique Channel Trough (MCT) strengthens (Barimalala et al., 2020). There is an increase in windspeed at the entrance to the Limpopo Valley as the trades are forced to accelerate due to the Bernoulli Effect. The circulation remains strong across the Botswana Plateau; rotating anticyclonically to enter northern South Africa. Winds associated with gaps in topography often remain strong downstream (e.g., Holbach & Bourassa, 2014; Macklin et al., 1990) and reach maximum intensity as the phase of the inertial oscillation progresses. The tendency for greatest windspeeds to occur around the Limpopo watershed in eastern Botswana from March-October may also relate to the absolute stability and associated nocturnal surface inversion, creating conditions conducive to mesoscale circulations (Tyson & Preston-Whyte, 1972).

Low-level windspeeds are strongest from August-November both in terms of their strength and spatial extent. Windspeeds remain strong through the Limpopo Valley in austral summer but are reduced in eastern and particularly southern Botswana from on average 13.1 m.s^{-1} to 11.4 m.s^{-1}, giving rise to a secondary clustering of core locations around the South Africa-Botswana-Zimbabwe border intersection, at the head of the Limpopo Valley. Jet strength and extent continue to reduce over the autumn, such that by May and June windspeeds >11.5 m.s^{-1} are only experienced over a localized area of eastern Botswana. The relative stationarity of the jet core through the annual cycle signals the control of topography on low-level windspeeds.

The vertical profile of windspeed at the jet core for each month is shown for strongest and weakest jet hours in Figure 3. Throughout the year, the nocturnal profile displays a clear low-level windspeed maximum underlying a region of high windspeed shear, giving the vertical profile a clear LLJ structure. Neither of the jet's core elements exist during the day, illustrating that it is clearly a nocturnal feature: low-level daytime windspeeds are typically less than half those achieved at night. Consequently there is no appreciable shear.

During austral winter, when low-level windspeeds are weakest, the jet is found closest to the surface (~300m agl); while still a clear low-level maximum (9.4 m.s^{-1} at its weakest in June), it is frequently eclipsed by mid-tropospheric windspeeds associated with the equatorward migration of the Subtropical Jet. Modal core height rises to ~500m agl as the jet strengthens in early spring. Jet height varies more over austral summer, when shear reduces slightly owing to stronger mid-tropospheric winds, but there remains a clear preference for a low-level nocturnal maximum throughout the year. Contrary to the nocturnal profiles, mean afternoon windspeed shows little variation across the annual cycle.

3.2. Diurnal Cycle

Figure 4 presents cross sections of mean October windspeed along and perpendicular to the jet axis at four-hourly intervals (equivalent plots for January, April and July are in Figures S1–S3). Windspeeds begin to increase in the early evening as turbulence-induced eddy viscosity in the boundary layer decreases and conditions become progressively stable. The jet is at its strongest at 23:00 when mean windspeeds at the core are 12.47 m.s^{-1}– an increase of 159% from their afternoon minimum values. It remains strong over the early hours of the morning, beginning to decay with the onset of surface heating. The diurnal cycle of windspeed along the Limpopo Valley and into central Botswana closely resembles the Blackadar (1957) mechanism regarded as classical LLJ formation (van de Wiel et al., 2010) whereby the jet is driven by an inertial oscillation resulting from the recoupling and decoupling of the boundary layer to the lower troposphere.

There is distinct zonal variation to the diurnal cycle which is present across all seasons and most visible in summer (Figures 4 and S1–S3). The onset of jet activity occurs first in the east over Mozambique and in the Limpopo Channel (Figure 4c), where the narrowing of the valley accelerates the flow. Jet activity then

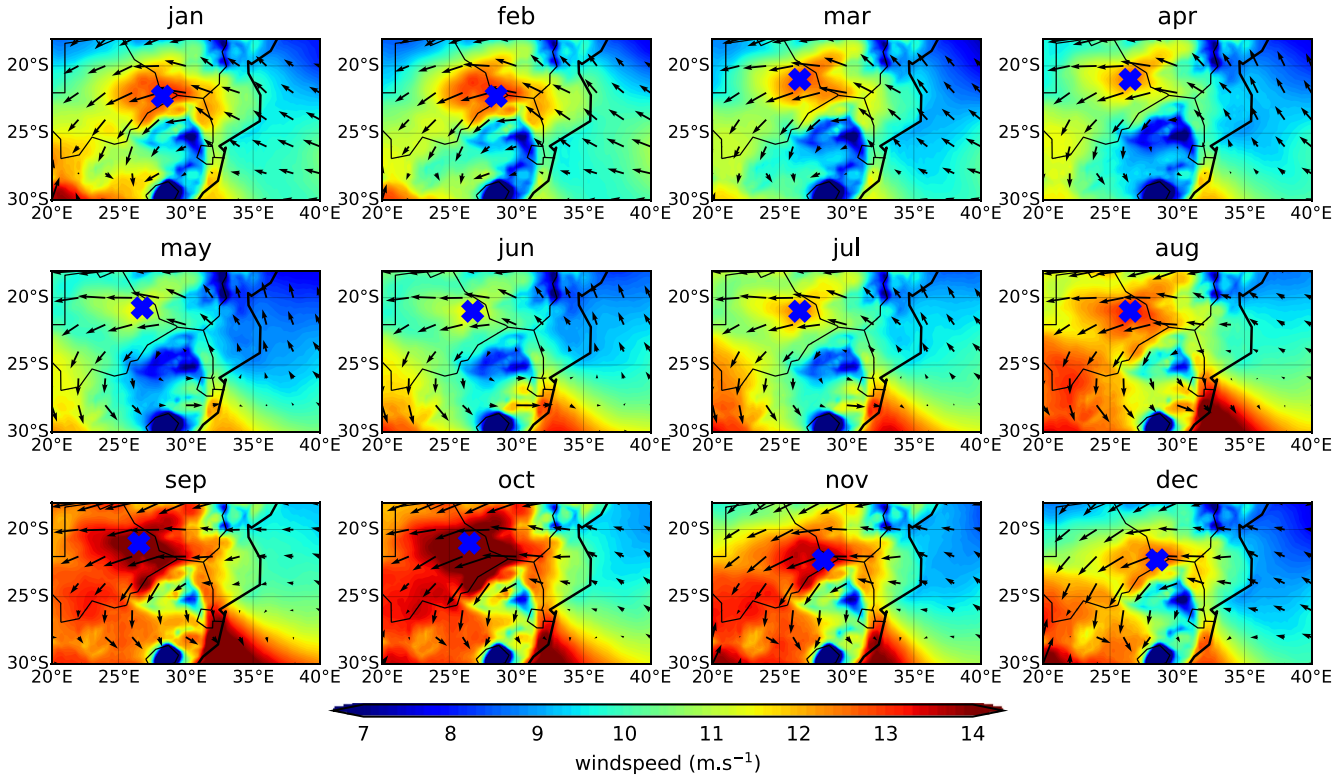

Figure 2. Monthly mean values of daily jet strength (maximum nocturnal windspeed over 925–800 hPa) in m.s^{-1}. Vectors are average monthly winds at the time and level selected as the jet maximum in each daily calculation. Crosses show jet core locations.

moves progressively westwards as the inertial oscillation reaches maximum intensity. Here, the very high absolute stability associated with frequent nocturnal surface inversions supports jet activity spreading over the Botswana Plateau–hence the jet remains strong beyond 07:00, until the inversion decays. However, this does not provide a complete explanation for the variation in timing across the jet axis; there is little appreciable change in stability over Mozambique from 23:00 to 07:00, but the jet weakens considerably from 03:00. It is possible that the observed gradient is the result of a combination of topographically driven mesoscale circulations interacting with the jet–such as katabatic breezes in tributary valleys. Idealized topography simulations could add greater nuance to understandings of precisely how topography affects the LLJ. Similar lags to peak jet activity across the jet axis have been observed in other locations (e.g., Jiménez-Sánchez et al., 2019), so the precise mechanisms responsible warrant further investigation.

The zonal gradient in timing along the jet axis partially explains the discrepancy in jet characteristics presented by Rife et al. (2010) and Algarra et al. (2019) (Table 1) beyond possible differences arising from the datasets used; it also appears to be a function of where they define the jet core. At 32.8°E, there is evidence for the early evening onset of jet activity reported by Rife et al. (2010), although ERA5 suggests jet structure persists here until at least 03:00. Equally, the later jet hours given by Algarra et al. (2019) of 00:00–05:00 are closer to the cycle seen over central Botswana but also underestimate persistence of the jet around dawn (Figure S1). Thus, some of the discrepancy relates to positioning of the jet core–which, in both studies, is considerably different to the site of maximum windspeed we find in any month in ERA5 (Figure 2). This is particularly true of Algarra et al. (2019) core location at 18°E, which is clearly to the west of the system even at maximum extent in October.

While the mean circulation over the Limpopo Basin is divergent throughout the year and convergent over the interior, it undergoes a clear diurnal cycle in association with the LLJ (Figure S4). Divergence across the basin is greatest when the rate of air accelerating through the Limpopo Channel is at its maximum, weakening during the daytime as eddy viscosity retards the wind. A similar cycle is evident over central

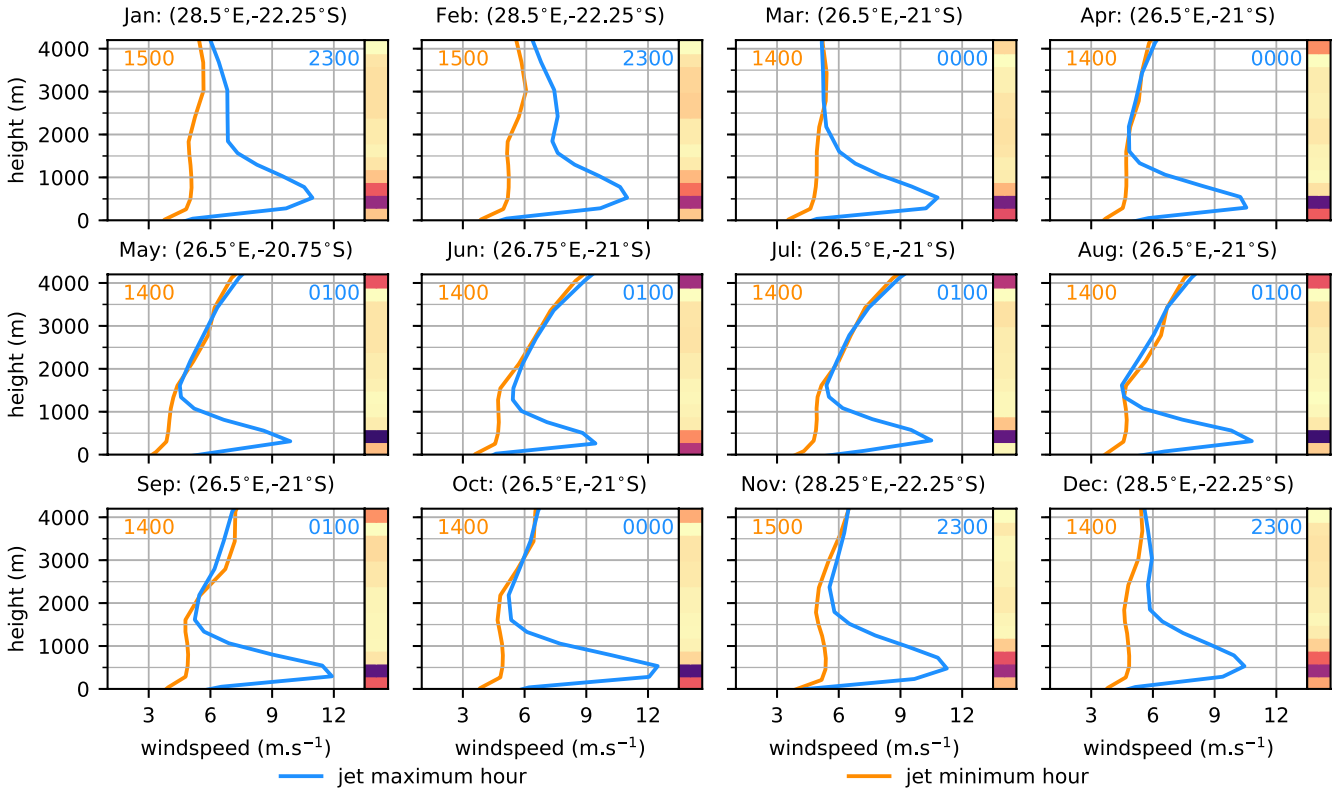

Figure 3. Monthly mean vertical profiles of windspeed in $m.s^{-1}$ at the jet core for each month when the jet is strongest (blue) and weakest (orange) during the day–corresponding to the times shown in each plot. Daily distribution of the vertical location of maximum windspeed at the jet maximum hour is displayed to the right of each profile, where deep red is the maximum.

Botswana where convergence dominates: convergence increases when the jet is active, ensuring a strong easterly feed from the Limpopo Valley. This weakens substantially during the day, giving way to patches of muted divergence (Figures S4b and S4i).

3.3. Annual Cycle

To explore drivers of the annual cycle of the Limpopo LLJ in greater detail, we compare the difference in geopotential height at 850 hPa across the Limpopo Basin with monthly average nocturnal maximum windspeed at the jet core (Figure 5). There is a strong positive relationship between the two variables ($r = 0.887$, $p < 0.0001$, $n = 12$), indicating that the height gradient across the basin acts as a first order control on the annual cycle of jet strength.

Geopotential height maps showing the seasonal evolution of the pressure gradient over southern Africa are presented in Figure S5. The clear minimum in jet strength over MJJ coincides with the development of the winter continental high centered over the Limpopo basin, which expands over the entire subcontinent in June. As the high weakens over the interior and shifts eastwards, the pressure gradient along the Limpopo Valley increases greatly, creating the unimodal peak in jet strength in October. As the high disappears in late spring, the geopotential height gradient decreases slightly but is maintained over summer by the Angola tropical and Kalahari heat lows, drawing low-level easterlies across the subcontinent. The flow over the Limpopo Basin becomes progressively southeasterly through the summer as the MCT strengthens to maximum intensity in February (Barimalala et al., 2020). With the weakening of the two continental low-pressure systems and simultaneous growth of the winter continental high, both the gradient and jet strength weaken from April to complete the annual cycle.

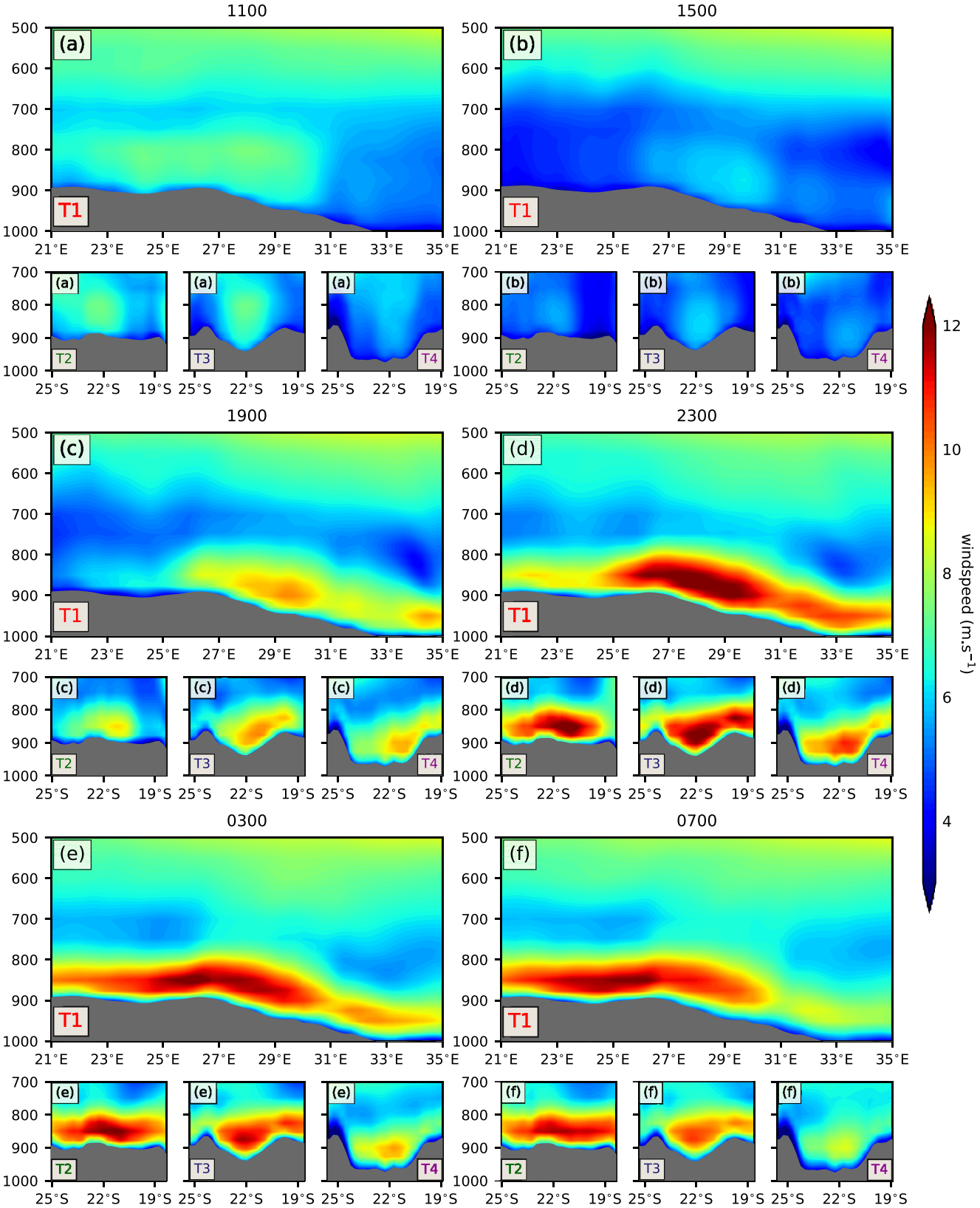

Figure 4. Longitude-height along the jet axis (large plot) and latitude-height along T2 (small left), T3 (small center) and T4 (small right) (Figure 1a) of mean October windspeed (m.s^{-1}) at (a) 1100; (b) 1500; (c) 1900; (d) 2300; (e) 0300 and (f) 0700.

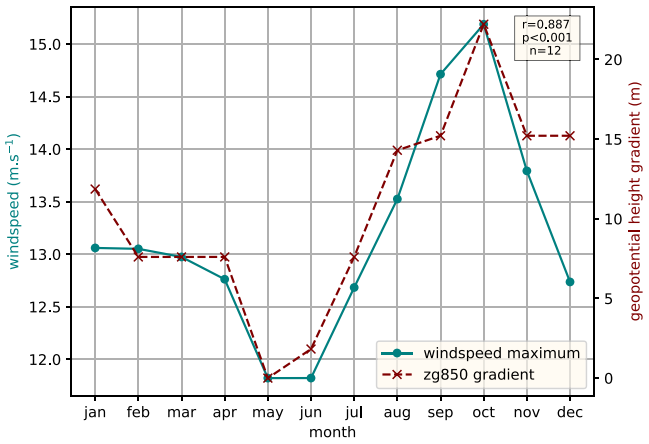

Figure 5. Annual cycle of average nocturnal maximum windspeed (m.s^{-1}) at the jet core (solid line) and the monthly mean geopotential height gradient along the jet axis (dashed line): taken as the difference in average geopotential height (850 hPa) over (33°E, 22°S–34°E, 23°S) and (25°E, 21.5°S–26°E, 22.5°S).

4. Variability of the Jet

This section considers variability of the jet at intraseasonal timescales after outlining the approach taken to measure daily jet strength.

4.1. Jet Criteria

In order to objectively consider variability of the Limpopo LLJ and its effects on regional climate on an event-by-event basis, a robust framework for detecting jet strength is needed to ensure analyses do not become biased by synoptic systems with high windspeeds that overwhelm the weaker detail of boundary layer oscillations. Hence, sampling by maximum windspeed alone is insufficient; confirming the circulation qualifies as a LLJ is an important first step. Despite a reasonable understanding of the processes leading to jet formation, there remains no set definition of a LLJ across the literature (Gimeno et al., 2016; Liu et al., 2014; Rife et al., 2010). Nevertheless, the two core elements of Blackadar's (1957) initial depiction of the Great Plains Jet–a significant windspeed maximum at a low level of the atmosphere accompanied by some element of shear to the vertical profile–remain common to every definition and are unequivocally visible across the Limpopo Basin in the climatological mean (Figures 3 and 4).

We therefore employ a series of hierarchical criteria based on these elements to verify the presence of a LLJ each day and categorize its strength, following the approach first used by Bonner (1968). In addition to stipulating minimum values for windspeed and vertical shear, we also impose a threshold considering the jet's diurnal variability given the pronounced cycle revealed in Section 3. The chosen thresholds were selected with reference to a large sample of daily vertical windspeed profiles. Testing with alternative thresholds revealed qualitatively similar results.

Days are sampled based on conditions at the jet core. Shear is measured as the difference in windspeed at jet height and the minimum value recorded over 800–650 hPa at the time when the jet is strongest. Diurnal variability refers to the magnitude of windspeed increase relative to the afternoon minimum recorded at jet height. First, as prevailing conditions over the basin are easterlies of some description throughout the year, days lacking an easterly zonal component are removed. The remaining days are then divided into one of three primary hierarchical categories as follows:

- Category A: Shear ≥8m.s^{-1} and diurnal variability ≥100%
- Category B: 4m.s^{-1} ≤Shear <8m.s^{-1} and diurnal variability between 50% and 99%
- Category 0: all remaining days failing to meet the criteria for categories A and B

Days in categories A or B are then subclassified into (i) if jet strength exceeds 15m.s^{-1} or (ii) if not.

These criteria are less stringent than those used by Bonner (1968) to characterize the Great Plains LLJ, but more so than in other subsequent studies that have used a similar approach (e.g., Marengo et al., 2004; Nicholson, 2016). Windspeed values presented here reflect the instantaneous nocturnal maximum across hourly data, so may differ from values reported in other studies that use time-averaged products, or those of a lower temporal resolution.

Figure 6 gives a visual representation of these categories: dividing the vertical profiles of days in October, when the jet is strongest, accordingly. The strongest events are divided across categories A(i) and B(i) (Figures 6a and 6d). Both classes have a distinct low-level maximum, although the rate of windspeed decrease above the jet core is greater in the former. This difference is more visible when the equivalent profiles are drawn for other months (not shown). Although weaker, jet structure is visible in the other classes in which a LLJ is identified (Figures 6b and 6e) – even for the 10th percentile of category B(ii) (the weakest category). Some unclassified days resemble jet structure, but these classes are marked by considerable variability throughout the vertical profile.

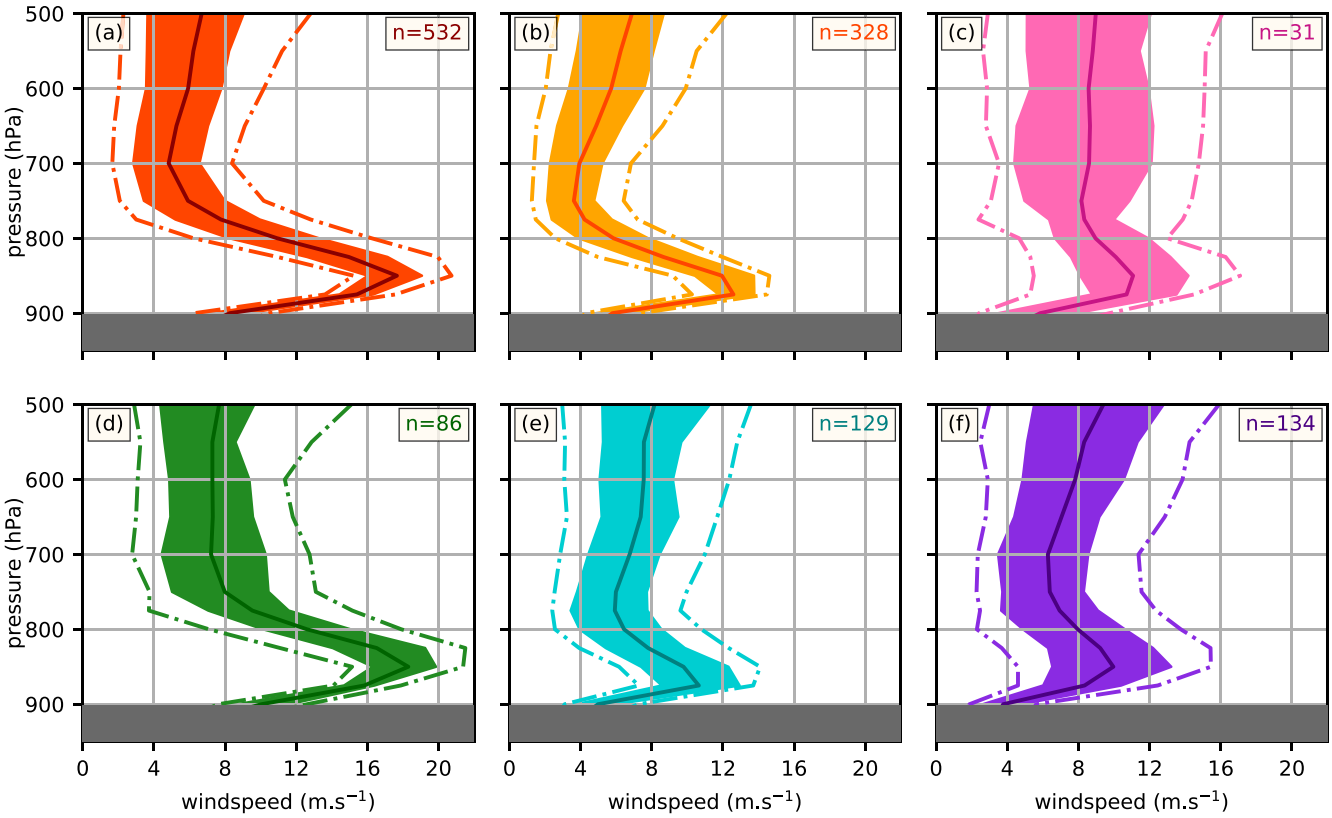

Figure 6. Vertical profiles of windspeed in m.s^{-1} at the jet core in October for (a) Category A(i) days (b) Category A (ii) (c) Category 0 (d) Category B(i) (e) Category B(ii) and (f) days where the low-level maximum lacks an easterly component. Solid, darker line represents the mean vertical profile for days in each class; shaded area depicts the 25th–75th percentiles of daily profiles. Dash-dotted lines show 10th and 90th percentiles.

4.2. Intraseasonal Variability in Jet Strength

The division of days across jet categories is shown in Table 2. The jet is a persistent feature of the circulation throughout the year that forms on 80.9% of days with a median strength of 13.9 m.s^{-1}. Such a high frequency of occurrence suggests that low-level divergence associated with the acceleration of the jet through the Limpopo Valley is likely to contribute to the basin's prevailing aridity, particularly during austral summer, when jet activity is strongest in the valley and rainfall contrast with the surrounding areas greatest (Figure 1c). Sampling based on the division of days across jet categories yields the same annual cycle seen in Section 3: Jet occurrence peaks in October (86.7%) when <3% of days with an easterly flow fail to meet the minimum requirements for shear and nocturnal acceleration. Total jet occurrence decreases gradually to a minimum in June (72.4%), but this difference is much more pronounced when considering the number of strong jet events, which decline sharply from their October peak. In austral summer this is compensated by an increase in days meeting the less stringent jet criteria, while in winter wind direction is slightly more variable. Perhaps unsurprisingly, early spring sees the greater number of extreme days, when ~10% of jet events achieve windspeeds in excess of 20m.s^{-1}.

To investigate the different synoptic settings that drive variability in jet strength, we consider geopotential height at 850 hPa in January (Figure 7). We focus on January for three reasons: (a) the distribution of days across jet categories is more even; (b) the amount of moisture imported by the jet is closer to its annual peak in February (Munday et al., 2021); (c) January is the center of the wet season (Figure 1d).

Days with the greatest windspeeds through the Limpopo Valley are associated with a ridging anticyclone centered on the east coast of South Africa (Figures 7a and 7d). Combined with a reduction in geopotential height over Botswana on Category A(i) days, this sharpens the pressure gradient and promotes SSE-SE flow over southern Mozambique. It is possible that the greater low-level synoptic disturbance reduces vertical

Table 2
Percentage of Days Comprising Each Jet Category

Month	Category A (i)	Category A (ii)	Category B (i)	Category B (ii)	Category 0	N-(W)-S	Total jet	Total non-jet	*Median windspeed ($m.s^{-1}$)*	*90th percentile windspeed ($m.s^{-1}$)*
Jan	14.8	27.7	6.9	34.4	12.1	4.1	**83.8**	**16.2**	*13.37*	*16.83*
Feb	12.5	24.4	9.0	35.2	15.8	3.1	**81.2**	**18.8**	*13.46*	*16.84*
Mar	20.9	31.5	7.4	23.4	9.3	7.6	**83.1**	**16.9**	*13.6*	*17.35*
Apr	18.5	37.2	6.3	21.9	7.2	8.8	**83.9**	**16.1**	*13.39*	*17.58*
May	12.6	38.5	4.8	22.8	5.9	15.5	**78.6**	**21.4**	*12.95*	*16.69*
Jun	11.7	28.4	6.1	26.2	10.1	17.5	**72.4**	**27.6**	*12.57*	*17.56*
Jul	19.8	26.4	9.8	19.9	9.0	15.2	**75.9**	**24.1**	*12.57*	*17.56*
Aug	28.1	29.5	7.3	13.5	5.9	15.8	**78.3**	**21.7**	*14.59*	*18.98*
Sep	36.8	28.6	7.2	9.5	3.7	14.2	**82.1**	**17.9**	*15.29*	*19.76*
Oct	42.9	26.5	6.9	10.4	2.5	10.8	**86.7**	**13.3**	*15.58*	*20.15*
Nov	28.3	22.3	7.7	25.1	7.5	9.1	**83.4**	**16.6**	*14.42*	*18.43*
Dec	16.8	29.0	5.8	30.3	10.8	7.3	**81.9**	**18.1**	*13.34*	*16.94*
Annual	**22.0**	**29.2**	**7.1**	**22.6**	**8.3**	**10.8**	**80.9**	**19.1**	***13.87***	***18.24***

Note. Median and 90th percentile windspeed values ($m.s^{-1}$) across jet days are also shown (italicized).

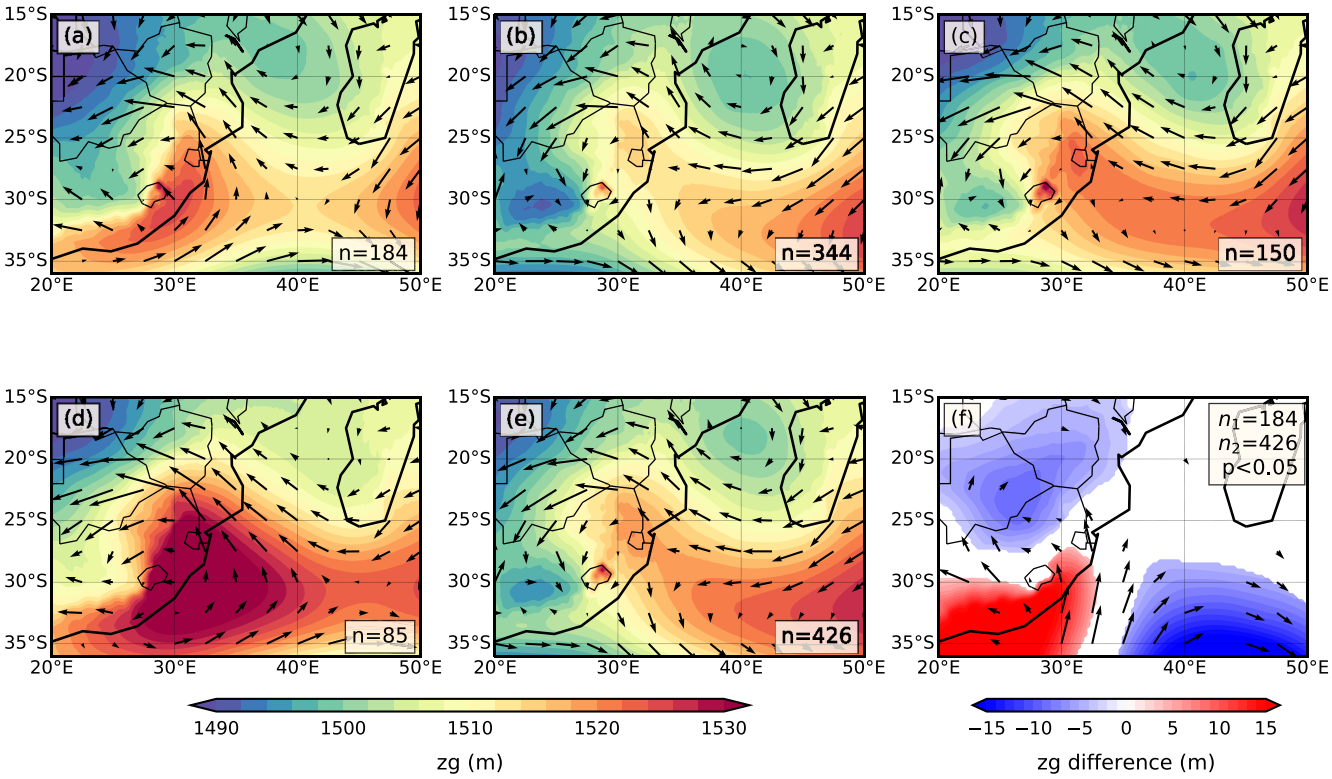

Figure 7. Composite means of daily geopotential height (850 hPa) for (a) Category A(i) days; (b) Category A(ii); (c) Unclassified easterlies; (d) Category B(i); (e) Category B(ii) in January. Panel (f) shows the difference between Category A(i) and B(ii) days, where differences are significant at 5% according to Students *t*-test.

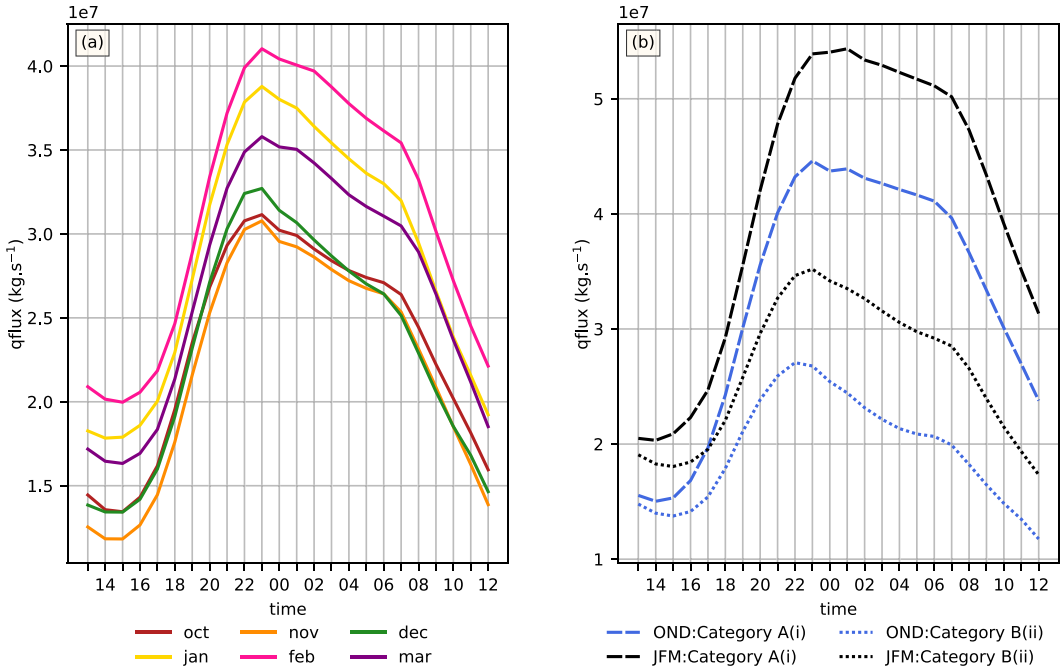

Figure 8. Average diurnal cycle of moisture flux (kg.s^{-1}) through the Limpopo Valley for: (a) October-March; (b) Category A(i) and B(ii) days averaged across OND and JFM.

shear on category B(i) days by perturbing conditions over South Africa such that the normal rhythm of boundary layer oscillations is interrupted. Such a mechanism could also reduce the diurnal variability of windspeeds by diminishing frictional forces on the daytime flow.

In contrast, weaker LLJs are associated with a westwards expansion of the Mascarene High, evidence of a trough over the southern South African coast and some suggestion of a deeper MCT increasing vorticity in the channel, deflecting flow from the Limpopo Channel (i.e., Figure 7b). There is little appreciable difference between the low-level synoptic setting of the weakest jet events (Figure 7e) and those that are unclassified (Figure 7c)—potentially reflecting a wider variability in synoptic setting across unclassified days.

5. Role in Water Vapor Transport

This section considers the role of the Limpopo LLJ in supplying moisture to the continental interior. It begins by examining the mean diurnal cycle of moisture transport from October to March (Figure 8).

In every summer month, there is a clear nocturnal maximum to moisture transported through the Limpopo Valley in phase with jet strength, peaking at 23:00. At this point, the rate of moisture transport is more than double the afternoon minimum. In each of the months considered, 72% (February)–75% (November) of the total water vapor transported through the Limpopo Valley occurs between 18:00 and 08:00. The annual cycle of moisture transport is evident; increasing over the early summer months to a maximum in February (Munday et al., 2021, Figure 1d) reflecting the general increase in specific humidity over the basin in late summer.

The amount of moisture advected through the Limpopo Valley is strongly influenced by jet strength throughout the wet season (Figure 8b): there is a substantial increase in moisture transport during the strongest jet events compared to the weakest. Over 18:00–08:00, this amounts to a total difference in water vapor of 1.04×10^{12} kg (1.02×10^{12} kg) in OND (JFM) transported through the valley. Although Category B(ii) events continue to show a nocturnal peak, the amplitude of the diurnal cycle is substantially greater for Category A(i) events such that the difference occurs primarily nocturnally (i.e., when the greatest difference in jet strength is felt). Moreover, while the rate of moisture flux decreases gradually from 23:00 with

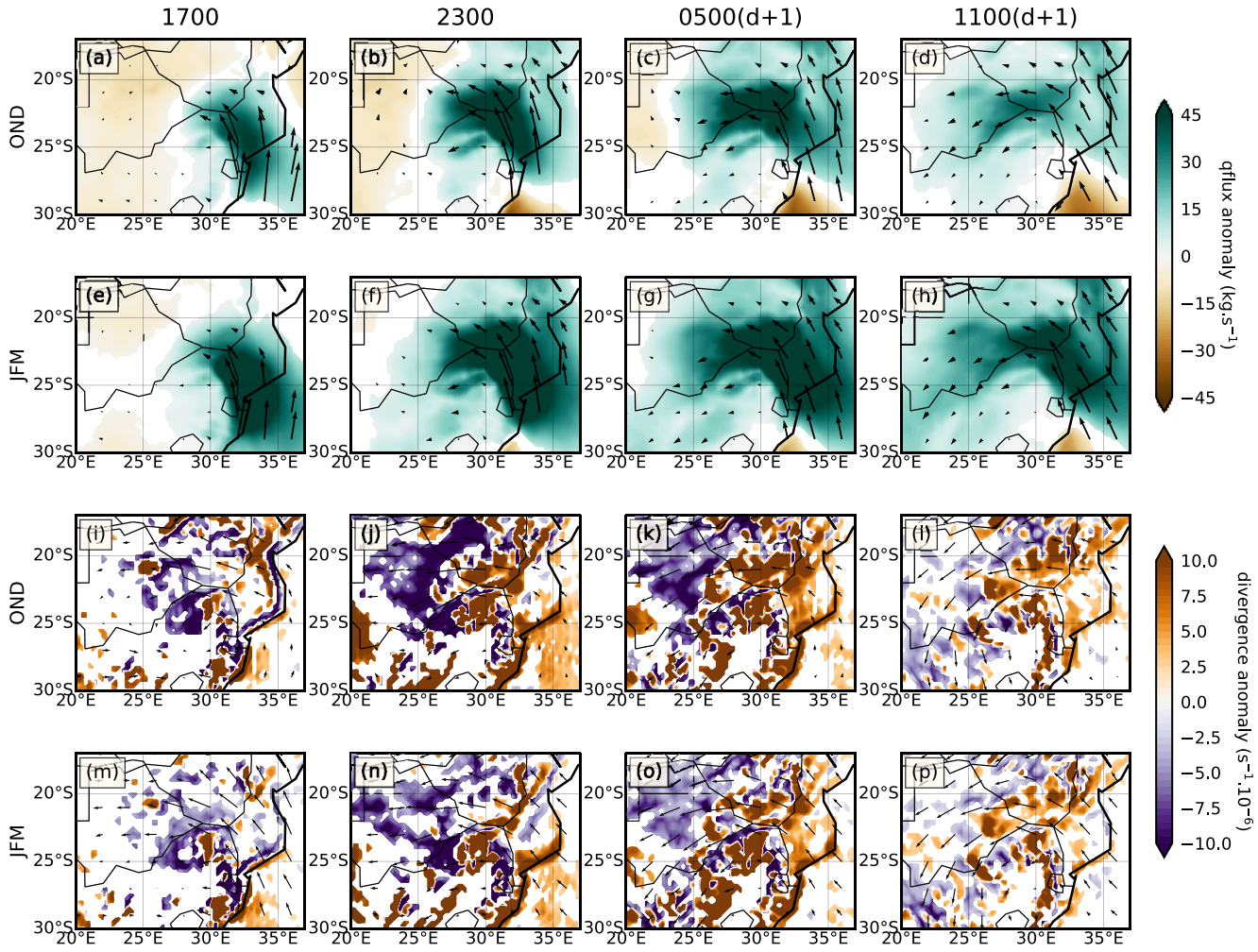

Figure 9. Difference in (a–h) moisture flux (kg.s^{-1}) integrated over surface-800 hPa and (i–p) horizontal divergence at 850 hPa (s^{-1}) between category A(i) and B(ii) days over eastern southern Africa for the early and late wet season. Vectors are the difference in the integral of q (u,v) (a–h) and difference in 850 hPa winds (i–p). In all instances, only differences significant at 5% based on Students t-test are shown. Times shown are at six-hourly intervals surrounding maximum jet intensity (second column), such that the right two columns show conditions the following calendar day.

the weakest events, it remains strong throughout the night until 07:00 with the strongest LLJs, decreasing sharply as jet activity decays with the onset of surface heating.

Figures 9a–9f show the increase in easterly moisture flux associated with the strongest jet events. The greatest difference is in the Limpopo Valley, particularly during OND, but it is symptomatic of a general increase in water vapor transport over a large area. The additional moisture flux is of southerly origin in the composite mean across the wet season, bound up with the ridging anticyclone responsible for strengthening the jet (Figure 7f) and as such enters the Limpopo Valley after traveling along the eastern escarpment (Figures 9a and 9e). As jet activity progresses westwards in the early hours of the morning, the additional moisture is no longer contained within the topography of the channel so disperses over the interior plateau. Consequently, a small but statistically significant ($p < 0.05$) increase in water vapor transport toward South Africa and SE Namibia occurs, persisting well into the following day. This is particularly visible later in the season, when the total moisture carried by the jet is greater.

With greater windspeeds across the basin, the strongest jet days are also associated with enhanced low-level divergence over the Mozambican floodplains and through the Limpopo Channel (Figures 9i–9p). This is particularly visible at night but likewise persists well into the following morning as winds are still returning to normal values. There is a substantial nocturnal enhancement of convergence in eastern Botswana

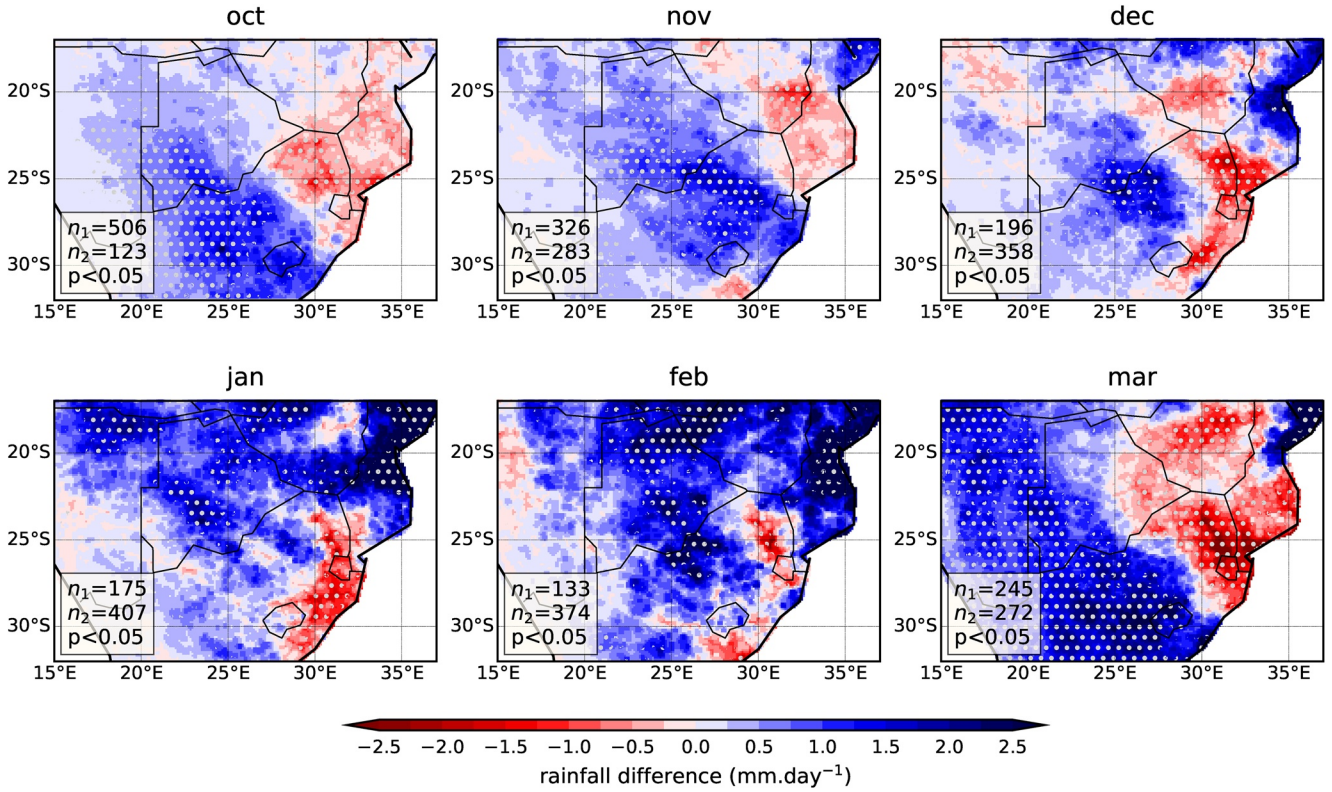

Figure 10. Difference in daily rainfall (CHIRPS; mm. day^{-1}) between the days that follow Category A(i) (strongest) jet events and B(ii) (weakest) events over the wet season (1981–2018). Stippling shows changes significant at 5% according to students t-test.

throughout the wet season, especially during OND (Figures 9j, 9k, 9n and 9o). Further downstream, there is also evidence of a small increase in convergence around the Botswana-South Africa border the following morning.

Therefore, as strong jet events induce dynamic changes conducive to rainfall downstream and the jet is clearly an important conduit of SWIO moisture to the continental interior, we briefly examine whether a difference exists in daily rainfall between the days following category A(i) compared to B(ii) jets (Figure 10).

A statistically significant ($p < 0.05$) increase in daily rainfall is generally observed across central southern Africa following the strongest compared to weakest jet events. In every month an increase is observed in Botswana–within, or immediately downstream of, the jet exit region, where increased convergence and the strong vertical shear of the jet profile create conditions favorable for rainfall. There is a suggestion that wetter conditions extend further across southern Africa, potentially due to the high influx of moisture delivered by a strong LLJ, but this is more variable across the season. Anomalies are particularly extensive in March, but it is unlikely this is solely attributable to the jet; rather, some synoptic disturbance existing on the days following strong events presumably promotes a widespread increase in rainfall, while the additional moisture supplied by the jet may contribute to the magnitude of increase.

Over the Limpopo Basin the rainfall response is more variable. Through the early summer months and March a relatively robust dipole pattern emerges to the sign of the anomaly; rainfall increases downstream while conditions are drier over southern Mozambique and the Limpopo Valley (Figures 10a–10c and 10f). Similar patterns have been documented for LLJs across the world on a range of timescales and are commonly attributed to a deficit in local moisture following strong export events (e.g., Cook & Vizy, 2010; Munday et al., 2021; Nascimento et al., 2016; Wang, 2007). It is possible that this mechanism is partially responsible for the drier conditions seen over the Limpopo Basin in the early summer. While a small increase in moisture transport across the Mozambique coast is still evident on the morning following strong jet events

(Figure 9d), anomalous moisture export through the Limpopo Valley exceeds the related increased import. Despite the additional flux through the Limpopo Valley the moisture is largely unavailable for rainfall given the simultaneous increase in divergence (Figures 9k and 9l). However, this pattern is not visible in January or February, when the Limpopo Basin experiences increases of rainfall similar in magnitude to those observed downstream. These anomalies are not statistically clear, suggesting a more variable response, but similarly wetter conditions are observed on the day of each jet event (not shown). This may relate to a weakly defined MCT and associated negative geopotential height anomalies south of the Mozambique Channel (Figures 7a and 7f); both of which are associated with a wetter JFM over the eastern subcontinent on interannual timescales (Barimalala et al., 2020).

6. Summary

This paper has developed the first climatology of the Limpopo LLJ, which had previously only been identified through isolated observational studies (summarized by Zunckel et al., 1996) and continental- (Munday et al., 2021) or global- (Algarra et al., 2019; Gimeno et al., 2016; Monaghan et al., 2010; Rife et al., 2010) scale studies. The vertical profile of windspeed in the Limpopo Basin exhibits a clear diurnal cycle, behaving according to the Blackadar (1957) mechanism of LLJ formation, with a distinct low-level maximum and considerable vertical shear nocturnally, but no evidence of jet structure during the afternoon. Hourly data from ERA5 demonstrates that there is a zonal gradient to the phase of jet activity, with onset, peak strength and demise occurring earliest over southern Mozambique before progressing westwards up-valley.

The jet exhibits a unimodal annual cycle, which is in phase with the pressure gradient between southern Mozambique and Botswana–as has been observed for many LLJs across the world (e.g., Liu et al., 2014; Muñoz et al., 2008; Patricola & Chang, 2017). Peak jet strength is achieved in October with average maximum windspeeds of 15.8 $m.s^{-1}$; 24% greater than in June. At this time, the winter continental high retreats eastwards such that it is centered over southern Mozambique, sharpening the pressure gradient with the interior. The development of the Angola tropical and Kalahari heat lows over the interior ensures a gradient is maintained over the core austral summer months, whereas the MJJ circulation is dominated by the subsequent expansion of the continental high over much of eastern southern Africa, translating into a substantial reduction in jet strength.

The Limpopo LLJ forms on 80.9% of days across the year and exhibits considerable variability on intraseasonal timescales. Greatest windspeeds are associated with a ridging anticyclone along the east South African coast sharpening the pressure gradient along the jet axis. There is some evidence to suggest that a stronger MCT may be associated with a weaker jet on both daily and seasonal timescales, potentially through a combination of increased vorticity in the Mozambique Channel and reduction of the pressure gradient, although this is less clear and requires further investigation.

Throughout the wet season, the jet plays a crucial role in importing SWIO moisture to the continental interior, in line with findings of previous studies (Algarra et al., 2019; Gimeno et al., 2016), giving the injection of water vapor into central southern Africa a distinct nocturnal lifecycle. This is important because the amount of warm, moist air advected from the SWIO has long been recognised as an important determinant for annual precipitation over the interior (Behera & Yamagata, 2001; Cook et al., 2004; D'Abreton & Lindesay, 1993; Hoell et al., 2017; Reason, 2017; Walker, 1990). Nocturnal water vapor transport associated with strong jets increases by 1.04×10^{12} kg (1.02×10^{12} kg) in OND (JFM) relative to weak events, strengthening moisture flux from the eastern coast of South Africa via the Limpopo Valley to the interior plateau.

Strong jet events create environments which are both dynamically and thermodynamically favorable for rainfall. Analysis of CHIRPS data on days following a strong LLJ confirms an increase in rainfall across much of the continental interior, centered on central Botswana associated with increased convergence and moisture availability. It seems unlikely that changes as widespread as those observed in some months are entirely the result of a strengthened LLJ, but this does not preclude the jet from having an influence on the magnitude of rainfall increase. Although infrequent, Blamey and Reason (2012) speculate that MCC occurrences over the interior during the summer months may be related to jet activity. Our findings support this assertion by demonstrating that a strong LLJ enhances nocturnal influx of moisture, promotes convergence

and ensures considerable shear to the vertical profile; effects which frequently implicate LLJs with MCC activity across the world (Stensrud, 1996). A full exploration of the dynamics of extreme jet events could help to unpick the relationship between the jet and rainfall extremes suggested by Monaghan et al. (2010).

Low-level divergence across the Limpopo Basin follows the diurnal cycle of windspeed, strengthening nocturnally–a relationship that holds true when considering variability of the jet at daily timescales. Given the association between jet-induced divergence and aridity observed elsewhere in Africa (Munday et al., 2021; Nicholson, 2016), coupled with the low number of days without a LLJ, it seems plausible that this mechanism contributes to the relative aridity of the Limpopo Basin, in addition to the presence of Madagascar reducing the impact of moisture-bearing trade winds and strengthening the MCT (Barimalala et al., 2018). In this light, what was once perceived as a 'problem climate' (Trewartha, 1981) is in fact so due to the presence of a feature which is key to supplying moisture to the interior of southern Africa. However, the relationship between jet strength and rainfall over southern Mozambique is not straightforward and warrants further attention: in the early summer months and March drying occurs following a strong LLJ, potentially due to an increase in moisture export, whereas during January and February the basin experiences increases in rainfall.

Given the role of the jet in delivering moisture to the southern African interior, future changes to the Limpopo Jet could have important consequences for regional climate. In addition to affecting rainfall, changes in water vapor concentration stand to modify the radiation budget. Investigating how the jet is represented by climate models is an important next step, particularly given the wet biases exhibited by most CMIP5 models over southern Africa (Munday & Washington, 2018). Our ability to understand jet dynamics and to evaluate model simulations of the jet would be greatly strengthened by direct observations of this persistent feature of the regional circulation. Getting these observations is a non-trivial task.

Data Availability Statement

ERA-5 data used in this study were accessed in 2020 and provided by the Copernicus Climate Change Service (https://cds.climate.copernicus.eu/cdsapp#!/home). Neither the European Commission nor ECMWF is responsible for any use that may be made of the Copernicus information or data it contains. USGS GTOPO30 global digital elevation model data were sourced from http://earthexplorer.usgs.gov/. CHIRPS data are available at https://data.chc.ucsb.edu/products/CHIRPS-2.0/.

Acknowledgments
The authors thank three anonymous reviewers for helpful comments that improved this manuscript. The first author is funded by the Met Office Academic Partnership (MOAP) and a small grant from St Edmund Hall, Oxford. Richard Washington is supported by the Natural Environmental Research Council (NERC)–UK Department for International Development (DFID) funded Improving Model Processes for African Climate (IMPALA) project (NE/M017206/1). Callum Munday is funded by the DFID REACH program (Aires Code 201880) and the NERC–DFID funded UMFULA project (NE/M020207/1).

References

Algarra, I., Eiras-Barca, J., Nieto, R., & Gimeno, L. (2019). Global climatology of nocturnal low-level jets and associated moisture sources and sinks. *Atmospheric Research*, *229*, 39–59. https://doi.org/10.1016/j.atmosres.2019.06.016

Allen, C. J. T., & Washington, R. (2014). The Low-Level Jet dust emission mechanism in the central Sahara: Observations from Bordj-Badji Mokhtar during the June 2011 fennec intensive observation period. *Journal of Geophysical Research: Atmosphere*, *119*(6), 2990–3015. https://doi.org/10.1002/2013JD020594

Barimalala, R., Blamey, R. C., Desbiolles, F., & Reason, C. J. C. (2020). Variability in the mozambique channel trough and impacts on Southeast African rainfall. *Journal of Climate*, *33*(2), 749–765. https://doi.org/10.1175/JCLI-D-19-0267.1

Barimalala, R., Desbiolles, F., Blamey, R. C., & Reason, C. (2018). Madagascar influence on the South Indian Ocean Convergence Zone, the Mozambique Channel Trough and southern African rainfall. *Geophysical Research Letters*, *45*(11), 380–389. https://doi.org/10.1029/2018GL079964

Behera, S. K., & Yamagata, T. (2001). Subtropical SST dipole events in the southern Indian Ocean. *Geophysical Research Letters*, *28*(2), 327–330. https://doi.org/10.1029/2000GL011451

Blackadar, A. K. (1957). Boundary layer wind maxima and their significance for the growth of nocturnal inversions. *Bulletin of the American Meteorological Society*, *38*(5), 283–290. https://doi.org/10.1175/1520-0477-38.5.283

Blamey, R. C., Middleton, C., Lennard, C., & Reason, C. J. C. (2017). A climatology of potentially severe convective environments across South Africa. *Climate Dynamics*, *49*(5–6), 2161–2178. https://doi.org/10.1007/s00382-016-3434-7

Blamey, R. C., & Reason, C. J. C. (2009). Numerical simulation of a mesoscale convective system over the east coast of South Africa. *Tellus A*, *61*(1), 17–34. https://doi.org/10.1111/j.1600-0870.2008.00366.x

Blamey, R. C., & Reason, C. J. C. (2012). Mesoscale convective complexes over Southern Africa. *Journal of Climate*, *25*(2), 753–766. https://doi.org/10.1175/JCLI-D-10-05013.1

Blamey, R. C., & Reason, C. J. C. (2013). The role of mesoscale convective complexes in Southern Africa summer rainfall. *Journal of Climate*, *26*(5), 1654–1668. https://doi.org/10.1175/JCLI-D-12-00239.1

Bonner, W. D. (1968). Climatology of the low level jet. *Monthly Weather Review*, *96*(12), 833–850. https://doi.org/10.1175/1520-0493(1968)096%3C0833:COTLLJ%3E2.0.CO;2

Cook, C., Reason, C. J. C., & Hewitson, B. C. (2004). Wet and dry spells within particularly wet and dry summers in the South African Summer Rainfall Region. *Climate Research*, *26*(1), 17–31. https://doi.org/10.3354/cr026017

Cook, K. H., & Vizy, E. K. (2010). Hydrodynamics of the Caribbean low-level jet and its relationship to precipitation. *Journal of Climate*, *23*(6), 1477–1494. https://doi.org/10.1175/2009JCLI3210.1

D'Abreton, P. C., & Lindesay, J. A. (1993). Water vapour transport over Southern Africa during wet and dry early and late summer months. *International Journal of Climatology*, *13*(2), 151–170. https://doi.org/10.1002/joc.3370130203

Farquharson, J. S. (1939). The diurnal variation of wind over tropical Africa. *Quarterly Journal of the Royal Meteorological Society*, *65*(280), 165–184. https://doi.org/10.1002/qj.49706528004

Funk, C., Peterson, P., Landsfeld, M., Pedreros, D., Verdin, J., Shukla, S., et al. (2015). The climate hazards infrared precipitation with stations—A new environmental record for monitoring extremes. *Scientific Data*, *2*, 150066. https://doi.org/10.1038/sdata.2015.66

Gimeno, L., Dominguez, F., Nieto, R., Trigo, R., Drumond, A., Reason, C. J. C., et al. (2016). Major mechanisms of atmospheric moisture transport and their role in extreme precipitation events. *Annual Review of Environment and Resources*, *41*, 117–141. https://doi.org/10.1146/annurev-environ-110615-085558

Hart, N. C. G., Reason, C. J. C., & Fauchereau, N. (2013). Cloud bands over southern Africa: Seasonality, contribution to rainfall variability and modulation by the MJO. *Climate Dynamics*, *41*(5–6), 1199–1212. https://doi.org/10.1007/s00382-012-1589-4

Hersbach, H., Bell, B., Berrisford, P., Biavati, G., Horányi, A., Muñoz-Sabater, J., et al. (2018a). *ERA5 hourly data on pressure levels from 1979 to presentCopernicus climate change services (C3S) climate data store (CDS)*. https://doi.org/10.24381/cds.bd0915c6

Hersbach, H., Bell, B., Berrisford, P., Biavati, G., Horányi, A., Muñoz-Sabater, J., et al. (2018b). *ERA5 hourly data on single levels from 1979 to presentCopernicus climate change services (C3S) climate data store (CDS)*. https://doi.org/10.24381/cds.adbb2d47

Hoell, A., Funk, C., Zinke, J., & Harrison, L. (2017). Modulation of the Southern Africa precipitation response to the El Nino Southern Oscillation by the subtropical Indian Ocean Dipole. *Climate Dynamics*, *48*(7), 2529–2540. https://doi.org/10.1007/s00382-016-3220-6

Holbach, H. M., & Bourassa, M. A. (2014). The effects of gap-wind-induced vorticity, the monsoon trough, and the ITCZ on East Pacific Tropical cycolgenesis. *Monthly Weather Review*, *142*(3), 1312–1325. https://doi.org/10.1175/MWR-D-13-00218.1

Jiménez-Sánchez, G., Markowski, P. M., Jewtoukoff, V., Young, G. S., & Stensrud, D. J. (2019). The orinoco low-level jet: An investigation of its characteristics and evolution using the WRF Model. *Journal of Geophysical Research: Atmosphere*, *124*(20), 10696–10711. https://doi.org/10.1029/2019JD030934

Liu, H., He, M., Wang, B., & Zhang, Q. (2014). Advances in low-level jet research and future prospects. *Journal of Meteorological Research*, *28*(1), 57–75. https://doi.org/10.1007/s13351-014-3166-8

Macklin, S. A., Bond, N. A., & Walker, J. P. (1990). Structure of a low-level jet over lower cook inlet, Alaska. *Monthly Weather Review*, *118*(12), 2568–2578. https://doi.org/10.1175/1520-0493(1990)118%3C2568:SOALLJ%3E2.0.CO;2

Marengo, J. A., Soares, W. R., Saulo, C., & Nicolini, M. (2004). Climatology of the low-level jet east of the Andes as derived from the NCEP-NCAR reanalyses: Characteristics and temporal variability. *Journal of Climate*, *17*(12), 2261–2280. https://doi.org/10.1175/1520-0442(2004)017%3C2261:COTLJE%3E2.0.CO;2

Monaghan, A. J., Rife, D. L., Pinto, J. O., Davis, C. A., & Hannan, J. R. (2010). Global precipitation extremes associated with diurnally varying low-level jets. *Journal of Climate*, *23*(19), 5065–5084. https://doi.org/10.1175/2010JCLI3515.1

Munday, C., & Washington, R. (2018). Systematic climate model rainfall biases over southern africa: Links to moisture circulation and topography. *Journal of Climate*, *31*(18), 7533–7548. https://doi.org/10.1175/JCLI-D-18-0008.1

Munday, C., Washington, R., & Hart, N. C. G. (2021). African low-level jets and their importance for water vapor transport and rainfall. *Geophysical Research Letters*, *48*(1), e2020GL090999. https://doi.org/10.1029/2020GL090999

Muñoz, E., Busalacchi, A. J., Nigam, S., & Ruiz-Barradas, A. (2008). Winter and summer structure of the caribbean low-level jet. *Journal of Climate*, *21*(6), 1260–1276. https://doi.org/10.1175/2007JCLI1855.1

Nascimento, M. G., Herdies, D. L., & Oliveira de Souza, D. (2016). The south american water balance: The influence of low-level jets. *Journal of Climate*, *29*(4), 1429–1449. https://doi.org/10.1175/JCLI-D-15-0065.1

Nicholson, S. (2016). The Turkana low-level jet: Mean climatology and association with regional aridity. *International Journal of Climatology*, *36*(6), 2598–2614. https://doi.org/10.1002/joc.4515

Nicholson, S. E. (2010). A low-level jet along the Benguela coast, an integral part of the Benguela current ecosystem. *Climatic Change*, *99*, 613–624. https://doi.org/10.1007/s10584-009-9678-z

Patricola, C. M., & Chang, P. (2017). Structure and dynamics of the Benguela low-level coastal jet. *Climate Dynamics*, *49*, 2765–2788. https://doi.org/10.1007/s00382-016-3479-7

Ramos, A. M., Blamey, R. C., Algarra, I., Nieto, R., Gimeno, L., Tomé, R., et al. (2019). From Amazonia to southern Africa: Atmospheric moisture transport through low-level jets and atmospheric rivers. *Annals of the New York Academy of Sciences*, *1436*(1), 217–230. https://doi.org/10.1111/nyas.13960

Rapolaki, R. S., Blamey, R. C., Hermes, J. C. & Reason, C. J. C. (2019). A classification of synoptic weather patterns linked to extreme rainfall over the Limpopo River Basin. *Climate Dynamics*, *53*(3), 2265–2279. https://doi.org/10.1007/s00382-019-04829-7

Rapolaki, R. S., Blamey, R. C., Hermes, J. C., & Reason, C. J. C. (2020). Moisture sources associated with heavy rainfall over the Limpopo River Basin, southern Africa. *Climate Dynamics*, *55*, 1473–1487. https://doi.org/10.1007/s00382-020-05336-w

Reason, C. J. C. (2017). *Climate of southern Africa*. https://oxfordre.com/climatescience/view/10.1093/acrefore/9780190228620.001.0001/acrefore-9780190228620-e-513

Rife, D. L., Pinto, J. O., Monaghan, A. J., Davis, C. A., & Hannan, J. R. (2010). Global distribution and characteristics of diurnally varying low-level jets. *Journal of Climate*, *23*(19), 5041–5064. https://doi.org/10.1175/2010JCLI3514.1

Singleton, A. T., & Reason, C. J. C. (2006). Numerical simulations of a severe rainfall events over the Eastern Cape coast of South Africa: Sensitivity to sea surface temperature and topography. *Tellus A: Dynamic Meteorology and Oceanography*, *58*(3), 335–367. https://doi.org/10.1111/j.1600-0870.2006.00180.x

Stensrud, D. J. (1996). Importance of low-level jets to climate: A review. *Journal of Climate*, *9*(8), 1698–1711. https://doi.org/10.1175/1520-0442(1996)009%3C1698:IOLLJT%3E2.0.CO;2

Thoithi, W., Blamey, R. C., & Reason, C. J. C. (2021). Dry spells, wet days, and their trends across southern Africa during the summer rainy season. *Geophysical Research Letters*, *48*, e2020GL091041. https://doi.org/10.1029/2020GL091041

Trewartha, G. T. (1981). *The Earth's problem climates* (2nd ed.). The University of Wisconsin Press.

Tyson, P. D., & Preston-Whyte, R. A. (1972). Observations of regional topographically-induced wind systems in natal. *Journal of Applied Meteorology*, *11*(4), 643–650. https://doi.org/10.1175/1520-0450(1972)011%3C0643:OORTIW%3E2.0.CO;2

Van de Wiel, B. J. H., Moene, A. F., Steeneveld, G. J., Baas, P., Bosveld, F. C., & Holtslag, A. A. M. (2010). A conceptual view on inertial oscillations and nocturnal low-level jets. *Journal of the Atmospheric Sciences*, *67*(8), 2679–2689. https://doi.org/10.1175/2010JAS3289.1

Vizy, E. K., & Cook, K. H. (2019). Observed relationship between the Turkana low-level jet and boreal summer convection. *Climate Dynamics*, *53*(7), 4037–4058. https://doi.org/10.1007/s00382-019-04769-2

Walker, N. D. (1990). Links between South African summer rainfall and temperature variability of the agulhas and benguela current systems. *Journal of Geophysical Research*, *95*(C3), 3297–3319. https://doi.org/10.1029/JC095iC03p03297

Wang, C. (2007). Variability of the Caribbean low-level jet and its relations to climate. *Climate Dynamics*, *29*, 411–422. https://doi.org/10.1007/s00382-007-0243-z

Washington, R., Todd, M. C., Engelstaedter, S., Mbainayel, S., & Mitchell, F. (2006). Dust and low-level circulation over the Bodélé Depression, Chad: Observations from BoDEx 2005. *Journal of Geophysical Research*, *111*, D03201. https://doi.org/10.1029/2005JD006502

Zunckel, M., Held, G., Preston-Whyte, R. A., & Joubert, A. (1996). Low-level wind maxima and the transport of pyrogenic products over southern Africa. *Journal of Geophysical Research*, *109*, D19–23755. https://doi.org/10.1029/95JD02602